

# Suppression of Autocrine and Paracrine Functions of Basic Fibroblast Growth Factor by Stable Expression of Perlecan Antisense cDNA

DAVID AVIEZER,<sup>1</sup> RENATO V. IOZZO,<sup>2</sup> DOUGLAS M. NOONAN,<sup>3</sup> AND AVNER YAYON<sup>1\*</sup>

*Department of Molecular Cell Biology, The Weizmann Institute of Science, Rehovot 76100, Israel<sup>1</sup>; Department of Pathology, Anatomy, and Cell Biology, Kimmel Cancer Center, Thomas Jefferson University, Philadelphia, Pennsylvania<sup>2</sup>; and Department of Chemical Carcinogenesis, Istituto Nazionale per la Ricerca sul Cancro, 16132 Genoa, Italy<sup>3</sup>*

Received 28 October 1996/Returned for modification 11 December 1996/Accepted 14 January 1997

**Heparan sulfate proteoglycans (HSPG) play a critical role in the formation of distinct fibroblast growth factor (FGF)-HS complexes, augmenting high-affinity binding and receptor activation. Perlecan, a secreted HSPG abundant in proliferating cells, is capable of inducing FGF-receptor interactions in vitro and angiogenesis in vivo. Stable and specific reduction of perlecan levels in mouse NIH 3T3 fibroblasts and human metastatic melanoma cells has been achieved by expression of antisense cDNA corresponding to the N-terminal and HS attachment domains of perlecan. Long-term perlecan downregulation is evidenced by reduced levels of perlecan mRNA and core protein as indicated by Northern blot analysis, immunoblots, and immunohistochemistry, using DNA probes and antibodies specific to mouse or human perlecan. The response of antisense perlecan-expressing cells to increasing concentrations of basic FGF (bFGF) is dramatically reduced in comparison to that in wild-type or vector-transfected cells, as measured by thymidine incorporation and rate of proliferation. Furthermore, receptor binding and affinity labeling of antisense perlecan-transfected cells with <sup>125</sup>I-bFGF is markedly inhibited, indicating that eliminating perlecan expression results in reduced high-affinity bFGF binding. Both the binding and mitogenic response of antisense-perlecan-expressing clones to bFGF can be rescued by exogenous heparin or perlecan. These results support the notion that perlecan is a major accessory receptor for bFGF in mouse fibroblasts and human melanomas and point to the possible use of perlecan antisense constructs as specific modulators of bFGF-mediated responses.**

Fibroblast growth factors (FGFs) are potent growth and angiogenic factors which are abundant in normal and malignant transformed cells (3). Basic FGF (bFGF) binds avidly to the glycosaminoglycan heparin and to heparan sulfates (HSs) found on cells and in the extracellular matrix. Studies on the mode of action of bFGF identified a novel role for heparin-like molecules in the formation of distinct bFGF-heparin complexes that are essential for FGF binding and activation of its tyrosine kinase receptor (1, 5, 10, 18, 24–28, 31–35, 38, 39, 42). In a search for candidate accessory receptors, we recently found that perlecan, the large basement membrane HS proteoglycan (HSPG), isolated from human fetal lung fibroblasts can induce high-affinity binding of bFGF to HS-deficient cells or to soluble FGF receptors (2). Heparin-dependent mitogenic and angiogenic activities of bFGF were also strongly augmented by perlecan. Interestingly, perlecan by itself could induce the formation of large blood vessels and an extensive network of fine capillaries in the rabbit ear model for angiogenesis. When complexed with bFGF, the angiogenic response to perlecan was further augmented, reaching overall neovascularization levels exceeding those obtained with immobilized heparin-bFGF complexes (2).

Perlecan, a component of all basement membranes, consists of three HS side chains linked to a large core protein of approximately 400 kDa (20, 29, 30). The protein core consists of five different domains, including an N-terminal HS attachment site which includes three SGD consensus sequences for HS glycanation, low-density lipoprotein receptor-like repeats, laminin A-like chains, epidermal growth factor (EGF)-like re-

gions, and a variant number of neural cell adhesion (N-CAM) immunoglobulin-like repeats (6, 16, 30). The variety of structural domains suggests multiple biological functions and possible interactions with other cell surface and basement membrane components. Expression of recombinant domain I of mouse perlecan in Chinese hamster ovary cells results in detectable modification of the recombinant protein by HS chains (22), indicating that domain I of perlecan has functional sites for GAG attachment.

The tissue localization of perlecan suggests that overexpression occurs at sites of tissue remodeling and active angiogenesis. Perlecan expression is evident in benign and in situ carcinomatous breast tissues (11). In invasive ductal and papillary carcinomas, perlecan is found to be upregulated and to surround the tumor blood vessels. Perlecan expression is dramatically enhanced in metastatic melanomas, and a correlation between perlecan upregulation and metastatic invasiveness of the tumor cells has been established (7). Moreover, angiogenic neovascularization is accompanied by a large increase in perlecan synthesized by prostate carcinoma cells (16). These observations suggest a tight association between perlecan expression and cell proliferation, tumor progression, and angiogenesis, which are all well correlated with bFGF activity. Furthermore, proliferation of human malignant melanoma cells, which are known to be dependent on their endogenous bFGF production (15), is inhibited by antisense oligonucleotides targeted against bFGF (4), demonstrating the crucial role for bFGF in the growth of human melanomas and the capacity to block such growth by an antisense approach.

In the present study, we demonstrate the effects of specific downmodulation of perlecan expression on the bFGF-mediated mitogenic response, basal growth, and bFGF binding in

\* Corresponding author. Phone: 972-8-934-2696. Fax: 972-8-934-4125. E-mail: liyayon@wiccmail.weizmann.ac.il.

mouse NIH 3T3 fibroblasts and human metastatic melanoma cells.

#### MATERIALS AND METHODS

**Plasmid construction.** The expression vector utilized for direction of mouse antisense perlecan expression was p $\beta$ APr-1-neo (14), kindly supplied by R. Takahashi (University of Kyoto, Kyoto, Japan). This vector places the target gene under the control of the strong  $\beta$ -actin promoter, and it has been previously shown to be effective in expression of antisense mRNA and specific inhibition of synthesis of endogenous molecules (14). For insertion of the cDNA encoding perlecan, minor modifications were made: the single *EcoRI* site (between the promoter and plasmid vector) was eliminated by cutting with *EcoRI*, filling in with Klenow fragment polymerase, and religating. An *EcoRI* restriction site was then inserted into the cloning site of p $\beta$ APr-1-neo by digestion with *Bam*HI and ligation with a linker containing the *EcoRI* recognition site and *Bam*HI-compatible overhangs. An *EcoRI* fragment containing clone 16 (30) was inserted into the new *EcoRI* site of the p $\beta$ APr-1-neo derivative. Clone 16 contains bases 1 to 1272 of the perlecan cDNA, including the 5' untranslated region, the start codon, and segments encoding domain I and a portion of domain II. The orientation of the inserted cDNA was determined by restriction enzyme digestion, and a plasmid with clone 16 in the antisense orientation, termed pBAAP (for plasmid  $\beta$ -actin antisense perlecan), was selected and expanded (see Fig. 1A). The final construct contained the  $\beta$ -actin promoter, first exon, first intron, and splice site of the second exon linked to clone 16 in an antisense orientation, followed by a simian virus 40 (SV40) polyadenylation site. A vector containing the neomycin resistance gene alone was used in experiments as a selection marker.

The cDNA encoding human perlecan bases 1 to 2013 was rescued from  $\lambda$ ZAP II (29). The insert cDNA was subcloned into the *EcoRI* site of the pBluescript KS plasmid. The expression vector utilized for direction of antisense perlecan expression was pcDNA3 (InVitrogen). Insertion of the perlecan cDNA in the antisense orientation into pcDNA3 was achieved by digestion with *EcoRI* and ligation with the perlecan insert from pBluescript. The antisense orientation of the inserted cDNA was verified by restriction enzyme analysis. The final construct contained sequences encoding domains I, II, and IIa and 400 bases of domain III in an antisense orientation.

**Cell lines expressing perlecan antisense cDNA.** NIH 3T3 cells were transfected with either the pBAAP plasmid or a p $\beta$ APr-1-neo plasmid, encoding the neomycin resistance gene, by electroporation (Gene Pulser; Bio-Rad). Transfected cells were selected and maintained in Dulbecco's modified Eagle's medium supplemented with 10% bovine calf serum (HyClone), 1% glutamine, and 0.8 mg of neomycin (Gibco) per ml. Human metastatic melanoma 501 cells (43) were transfected with the pcDNA3 expression vector, encoding human perlecan in the antisense orientation and the neomycin resistance gene, by electroporation. Transfected cells were selected and maintained in RPMI 1640 supplemented with 10% fetal calf serum (HyClone), 1% glutamine, and 1 mg of neomycin (Gibco) per ml. Individual clones of both cell lines showing G418 resistance were screened for perlecan expression by dot blot analysis with an anti-mouse or anti-human perlecan antibody accordingly.

**Northern blot analysis.** Northern blot analysis was performed on RNA (10  $\mu$ g) isolated from transfected and untransfected NIH 3T3 cells using the Tri-reagent RNA extraction solution (Molecular Research Center, Cincinnati, Ohio). Perlecan transcripts were detected with a  $^{32}$ P-labeled probe (nucleotides 1 to 1272) from mouse perlecan cDNA (30). Expression of glyceraldehyde-3-phosphate dehydrogenase was used in order to normalize the quantity of RNA loaded in each well.

**Immuno-dot blot analysis for perlecan.** Dot blot analysis was performed by collecting 400  $\mu$ l of conditioned medium from cultures of transfected and wild-type cells and absorbing it on nitrocellulose by using a dot blotter apparatus (Schleicher & Schuell). The blots were incubated with either an anti-mouse perlecan antibody (20) (kindly provided by Koji Kimata, Aichi Medical University, Aichi, Japan), an anti-syndecan-1 antibody (37) (kindly provided by M. Bernfield, Harvard Medical School, Boston, Mass.), or an anti-human perlecan antibody (kindly provided by Guido David, Center for Human Genetics, Leuven, Belgium). Incubation was carried out for 1 h at 24°C in Tris-buffered saline (10 mM Tris [pH 7.4], 150 mM NaCl) containing 10% low-fat milk and 1% ovalbumin. Subsequently, the blot was reacted for 45 min at room temperature with horseradish peroxidase-conjugated protein A and visualized by fluorography (ECL; Amersham).

**Immunofluorescence staining.** Monolayers of wild-type or antisense perlecan-transfected NIH 3T3 cells were grown on glass coverslips and fixed with 3% paraformaldehyde. The coverslips were incubated with the antiperlecan antibodies at a 1:40 dilution for 1 h at 37°C. After several washes with phosphate-buffered saline (PBS), antibody-antigen complexes were detected with fluorescein-conjugated anti-rabbit immunoglobulin G antibody (Sigma) and visualized by fluorescence microscopy (Zeiss).

**Stimulation of DNA synthesis in NIH 3T3 cells.** NIH 3T3 cells were grown in medium containing 10% fetal calf serum in 24-well plates to near confluence. The cells were then grown in serum-free medium for 24 h, after which they were added 10 ng of bFGF per ml and increasing concentrations of heparin. After 18 h of incubation at 37°C, the cells were then pulsed with 5  $\mu$ Ci of [ $^3$ H]thymidine per

ml for 6 h at 37°C, after which they were washed twice with PBS, incubated with a 5% trichloroacetic acid solution for 20 min, and then extracted with 0.1 N NaOH. Incorporation of radioactivity was determined in a beta counter (Packard).

**bFGF-induced cell proliferation of wild-type and perlecan antisense cDNA-expressing melanoma cells.** Wild-type and perlecan antisense cDNA-transfected melanoma cells were plated at  $2 \times 10^3$  per well in 24-well dishes. The cells were grown in serum-free RPMI 1640 supplemented with 1% glutamine and 1 mg of neomycin (Gibco) per ml for 7 days in the presence or absence of bFGF (10 ng/ml) and then counted at the indicated intervals.

**Binding of  $^{125}$ I-bFGF to cells.** High-affinity binding of bFGF to cells was performed as described previously (42). Briefly, low-affinity-bound bFGF was released from the cell surface by a 5-min incubation with a cold solution consisting of 1.6 M NaCl and 20 mM HEPES (pH 7.4). High-affinity-bound bFGF was determined by extraction in 2 M NaCl-20 mM acetate buffer (pH 4.0) and subsequent counting in a gamma counter.

**Cross-linking of radiolabelled bFGF to cells.** Confluent monolayers of wild-type NIH 3T3 and antisense perlecan-expressing cells were grown in six-well plates. Binding of  $^{125}$ I-bFGF to the cells was carried out as described above. After 90 min, disuccinylimidyl suberate (Pierce Chemical Co.) in dimethyl sulfoxide was added to a final concentration of 0.15 mM and the cells were incubated for 30 min at room temperature. The cells were lysed in 0.1 ml of lysis buffer (20 mM HEPES [pH 7.5], 150 mM NaCl, 10% glycerol, 1% Triton X-100, 1.5 mM MgCl<sub>2</sub>, 1 mM EGTA, 1 mM phenylmethylsulfonyl fluoride, 1  $\mu$ g of aprotinin/ml, 1  $\mu$ g of leupeptin/ml), and the lysates were incubated for 10 min on ice. The cell lysates were cleared by centrifugation (12,000  $\times$  g, 15 min, 4°C), boiled for 5 min in sample buffer (50 mM Tris [pH 6.8], 25% glycerol, 6%  $\beta$ -mercaptoethanol, 4% sodium dodecyl sulfate [SDS], 1 mM EDTA, 10% bromophenol blue), and loaded onto an SDS-7.5% polyacrylamide gel. After electrophoresis, the gel was dried and exposed to X-ray film for 36 h.

**Metabolic labeling of cells with sulfate.** Cells were metabolically labeled with 50  $\mu$ Ci of [ $^{35}$ S]sulfate (DuPont NEN) for 3 days and subsequently lysed as described previously (22). Total cell lysates were subjected to immunoprecipitation with anti-syndecan-1 antibody or antiperlecan antibody prebound to protein A (Pierce). Total cell lysates and immunoprecipitates were washed three times with PBS and counted in a beta counter (Packard).

**Western blot analysis for FGF receptor 1.** Confluent wild-type and antisense perlecan-expressing NIH 3T3 cells grown in 65-mm-diameter plates were lysed as described above and incubated with 50  $\mu$ l of wheat germ agglutinin beads (Pierce) for 12 h at 4°C. The precipitates were washed three times with HNTG (20 mM HEPES [pH 7.5], 150 mM NaCl, 10% glycerol, 1% Triton X-100), separated on an SDS-7.5% polyacrylamide gel, and transferred onto nitrocellulose. The blot was incubated with a polyclonal antibody to FGF receptor 1 for 1 h at 4°C in Tris-buffered saline (10 mM Tris [pH 7.4], 150 mM NaCl) containing 10% low-fat milk, reacted for 45 min at room temperature with horseradish peroxidase-conjugated protein A, and visualized by fluorography (ECL; Amersham).

## RESULTS

**Expression of perlecan antisense cDNA in mouse NIH 3T3 cells and human metastatic melanoma 501 cells.** NIH 3T3 mouse fibroblast cells, which normally are capable of binding and responding to bFGF (41) and endogenously express perlecan (16), were transfected with the expression vector designated pBAAP containing nucleotides 1 to 1272 of the mouse perlecan gene (30) in the opposite orientation (Fig. 1A). Neomycin-resistant clones were selected and tested for perlecan expression. Several stable cell lines were isolated, of which three were further propagated and designated mPAS-1, mPAS-2, and mPAS-8 (for mouse perlecan antisense). A neomycin-resistant clone transfected with the control vector (designated NIH neo) exhibited normal perlecan levels and served as a positive control throughout this work. Transfection and selection were repeated twice. Clones sharing similar characteristics were isolated in both rounds. The effect of transfection with mouse perlecan antisense cDNA on expression of perlecan mRNA was determined by Northern blot analysis performed on RNA isolated from transfected and untransfected NIH 3T3 cells (Fig. 1B). Perlecan expression is dramatically reduced in the transfected clones, and the ~12.7-kb perlecan transcript could be detected only in the untransfected or vector-transfected NIH 3T3 cells.

Human metastatic melanoma 501 cells, which bind and respond to bFGF (15, 43) and endogenously express perlecan

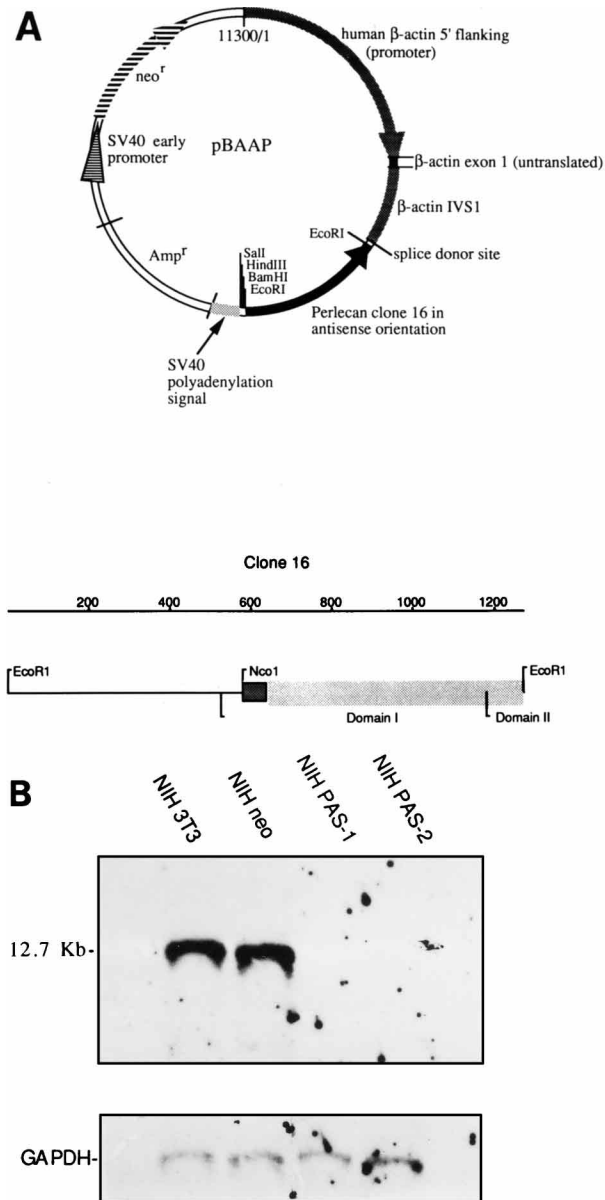


FIG. 1. Expression of perlecan mRNA in NIH 3T3 cells transfected with mouse perlecan antisense cDNA. (A) Schematic representation of the pBAAP construct. The plasmid contains the  $\beta$ -actin promoter and clone 16 bases 1 to 1272 of the mouse perlecan cDNA, including the 5' untranslated region and segments encoding domain I and a portion of domain II in an antisense orientation, followed by an SV40 polyadenylation site. In addition, the vector contains the neomycin resistance gene driven by the SV40 early promoter as a selectable marker. (B) Northern blot analysis of total RNA (10  $\mu$ g) isolated from wild-type and pBAAP-transfected NIH 3T3 cells. A radiolabeled probe derived from perlecan cDNA (nucleotides 1 to 1272) was used to detect perlecan mRNA levels. Lanes: 1, NIH 3T3 cells; 2, a neomycin-resistant NIH 3T3 clone; 3 and 4, perlecan antisense clones PAS-1 and PAS-2, respectively. Expression of glyceraldehyde-3-phosphate dehydrogenase (GAPDH) was used in parallel in order to control the total RNA quantity loaded in each well.

(16), were transfected with an expression vector containing nucleotides 1 to 2013 of the human perlecan gene (29) in an antisense orientation. Neomycin-resistant clones were selected and tested for perlecan expression. Several stable cell lines were isolated, of which three were further propagated and designated hPAS-1, hPAS-4, and hPAS-7 (for human perlecan

antisense). In addition, the mouse perlecan antisense construct was transfected into human melanoma cells as a control.

**Selective reduction in perlecan proteoglycan levels in NIH 3T3 and human melanoma cells expressing perlecan antisense cDNA.** Conditioned medium was collected from the antisense- and vector-transfected NIH 3T3 cell line cultures and tested by an immunoblot assay using polyclonal antibodies against mouse perlecan (20). As can be seen in the upper panel of Fig. 2A, conditioned medium from wild-type cells gave a clear immunoreaction to perlecan. Similarly, the antiperlecan antibodies identified perlecan purified from a mouse Engelbreth-Holm-Swarm tumor at levels similar to those of wild-type NIH 3T3 cells. However, all three cell lines that had been transfected with perlecan antisense cDNA produced minute levels of perlecan protein. In order to determine whether the perlecan antisense cDNA transfection had any effect on other proteins and proteoglycans in the cells, we measured the expression levels of the protein syndecan-1. As can be seen in Fig. 2A (middle panel), identical amounts of syndecan-1 are expressed in PAS-transfected and wild-type NIH 3T3 cells by antibodies specific for mouse syndecan-1 (37).

Conditioned medium collected from cultures of the human melanoma antisense-cDNA-transfected cells was similarly tested, this time with monoclonal antibodies specific to human perlecan (1). As can be seen in Fig. 2A (lower panel), both conditioned medium from wild-type cells and perlecan purified from human fetal lung fibroblasts reacted with the antibodies. However, human cell lines that had been transfected with the human perlecan antisense cDNA exhibited very low levels of perlecan protein. Human melanoma cells transfected with the mouse perlecan antisense construct, on the other hand, did not show any significant decrease in perlecan expression, indicating the specificity of the antisense approach, as the homology between the murine and human genes in these domains is only 68%. Taken together, these results indicate that perlecan antisense cDNA transfection can remarkably reduce the level of perlecan protein, in a specific manner, in both mouse fibroblasts and human melanoma cells.

To verify that perlecan antisense cDNA expression did not affect total or nonspecific proteoglycan sulfation levels, which in turn might hamper FGF receptor functions, wild-type and perlecan antisense cDNA-expressing NIH 3T3 cells were metabolically labeled with [ $^{35}$ S]sulfate and analyzed for total [ $^{35}$ S]sulfate incorporation into both the syndecan-1 and perlecan-associated glycosaminoglycans. Wild-type and mPAS-1 NIH 3T3 cells exhibited identical total cell sulfate incorporation levels (Fig. 2B). Similar  $^{35}$ S levels are found to be associated with syndecan-1 isolated from either wild-type or antisense-cDNA-transfected cells (Fig. 2B), indicating that the antisense-cDNA-expressing cells are capable of normal proteoglycan expression and sulfation. Perlecan immunoprecipitated from wild-type NIH 3T3 cells exhibits 10-fold higher  $^{35}$ S counts than that isolated from mPAS-1 cells (Fig. 2B), in agreement with the specific reduction in perlecan core protein production.

**Immunostaining for perlecan of wild-type and perlecan antisense cDNA-expressing cells.** In order to unequivocally demonstrate reduced perlecan expression and extracellular deposition in the selected clones, we stained monolayers of wild-type and perlecan antisense cDNA-transfected NIH 3T3 and melanoma cells with the polyclonal anti-mouse perlecan and monoclonal anti-human perlecan antibodies, respectively. Wild-type NIH 3T3 cells stained intensely for perlecan, which is found to be concentrated mainly in the extracellular spaces surrounding the cells (Fig. 3A and B). In contrast, perlecan antisense cDNA-transfected fibroblasts (mPAS-1) failed to ex-

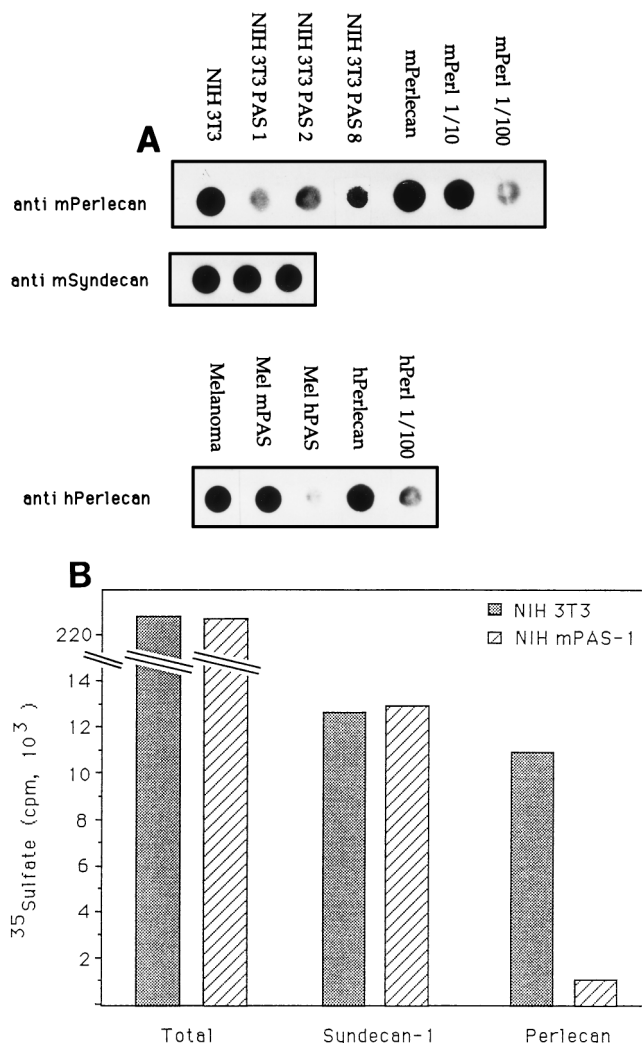


FIG. 2. Effects of perlecan antisense cDNA transfection on perlecan and syndecan-1 proteoglycan expression and sulfation. (A) Immunoblot of perlecan secreted from cells expressing perlecan antisense cDNA. Conditioned medium from cultures of wild-type NIH 3T3 cells (upper panel) or human melanoma (Mel) cells (lower panel), and from cultures of these cells after transfection with mouse or human perlecan antisense cDNA constructs, was absorbed onto nitrocellulose membranes. The membranes were blotted with polyclonal antibodies against mouse perlecan or with monoclonal antibodies against human perlecan, respectively. As a positive control, serial dilutions of mouse perlecan purified from a mouse Engelbreth-Holm-Swarm tumor or human perlecan purified from fetal lung fibroblasts were used (mPerlecan [mPerl] and hPerlecan [hPerl], respectively). The NIH 3T3 cell blot was also reacted with anti-mouse syndecan-1 antibodies (anti mSyndecan). (B) Effect of perlecan antisense cDNA transfection on levels of perlecan, syndecan-1, and total proteoglycan sulfation. Wild-type and transfected NIH 3T3 cells were metabolically labeled with [<sup>35</sup>S]sulfate for 3 days and subsequently lysed. Total cell lysates were counted and subjected to immunoprecipitation with anti-syndecan-1 or antiperlecan antibodies prebound to protein A. The immunoprecipitates were washed three times with PBS and counted in a beta counter.

hibit significant extracellular perlecan staining (Fig. 3D and E), in agreement with the marked reduction in perlecan mRNA and protein expression.

Wild-type metastatic melanoma 501 cells stained intensely for perlecan with anti-human perlecan monoclonal antibodies (2). In these cells, perlecan is found to be more evenly distributed on the cell surface (Fig. 3C), similar to the distribution found in human colon carcinoma cells (17). Perlecan antisense cDNA-transfected melanoma cells exhibit significantly re-

duced cellular perlecan staining (Fig. 3F), in agreement with the marked reduction in protein expression (Fig. 2). Some unexpected staining was noticed in the cell nuclei of both cell types; this may represent nuclear perlecan-like molecules or a nonspecific reaction with the antibodies.

**bFGF-induced cell proliferation is attenuated in perlecan antisense cDNA-expressing cells.** In order to characterize the biological consequences of reduced perlecan expression, we tested the ability of bFGF, a potent mitogen for fibroblasts (3) and an autocrine factor for melanoma cells (4, 15), to induce cell proliferation in antisense perlecan-expressing cells. Since perlecan from human fetal lung fibroblasts was shown to augment bFGF binding and activation (1), we hypothesized that cells in which perlecan expression is abated may have an attenuated response to bFGF. The rate of proliferation of parental NIH 3T3 cells, as demonstrated in Fig. 4A, is indeed greatly enhanced by the addition of bFGF to the growth medium. The rate of proliferation of parental human metastatic 501 melanoma cells (Fig. 4B) is also greatly enhanced by the addition of bFGF to the growth medium. However, cells expressing perlecan antisense cDNA hardly respond to bFGF, with overall proliferation rates similar to those of untreated wild-type cells (Fig. 4A and B). This effect is specific, as transfection of these human cells with the mouse perlecan antisense construct does not affect their response to bFGF (Fig. 4B), in agreement with their unchanged level of endogenous perlecan as demonstrated by the immunoblot analysis (Fig. 2A). Taken together, these results demonstrate that at reduced perlecan expression levels, bFGF activity is markedly inhibited in both NIH 3T3 and melanoma cells. The basal growth rates, however, of both parental and perlecan antisense cDNA-expressing cells are similar, indicating that the observed differential effect is bFGF specific.

**Exogenous heparin can reconstitute bFGF-induced cell proliferation in perlecan antisense cDNA-expressing cells.** The mitogenic response of cells to bFGF is absolutely dependent on the presence of a competent HSPG (1, 24, 27, 41). We therefore set up an experiment to determine whether heparin can restore the attenuated biological mitogenic effect of bFGF in perlecan-deficient fibroblasts. DNA synthesis measured by a thymidine incorporation assay (Fig. 4C) demonstrates that the perlecan antisense cDNA-expressing clone PAS-1 responds to bFGF only in the presence of exogenous heparin or perlecan. This is in contrast to wild-type or neomycin-resistant NIH 3T3 cells, which exhibit a clear mitogenic response to bFGF independent of exogenous heparin or HS. Perlecan or heparin alone has no effect on the mitogenic response of either cell type, indicating the crucial role of an appropriate bFGF-HS complex in the biological response to bFGF.

**Reduced bFGF binding to perlecan antisense cDNA-transfected cells.** Since cells expressing antisense perlecan did not exhibit the expected biological response to bFGF, we wished to determine whether this effect is caused by impaired bFGF-receptor binding. Direct binding of [<sup>125</sup>I]-bFGF to the different cell lines at saturating concentrations demonstrates that bFGF can bind with high affinity to FGF receptors on wild-type and neomycin-resistant NIH 3T3 cells but not to the antisense cDNA-expressing clones (Fig. 5A). A direct correlation between the level of perlecan expression (Fig. 2A) and the ability of the cells to bind bFGF is noticeable, as clone PAS-8, which expresses moderate levels of perlecan, is capable of binding bFGF accordingly. Similarly, bFGF can bind with high affinity to wild-type human melanoma cells or to human melanoma cells transfected with the mouse antisense construct, but it binds with much less affinity to melanoma cells expressing the human perlecan antisense cDNA (Fig. 5B). These results

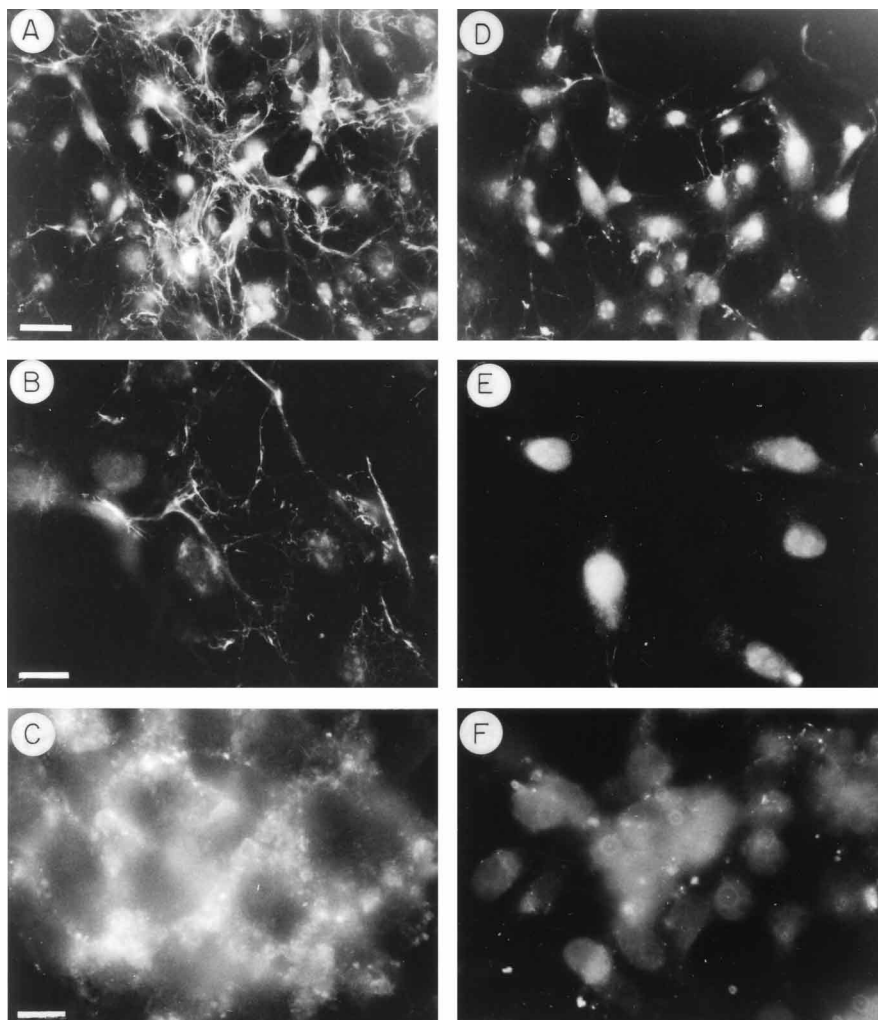


FIG. 3. Immunofluorescence staining for perlecan of wild-type and perlecan antisense cDNA-transfected NIH 3T3 cells. Monolayers of NIH 3T3 cells and NIH PAS-1 cells were stained with the polyclonal anti-mouse perlecan antibody. Antibody-antigen complexes were detected with fluorescein-conjugated anti-rabbit immunoglobulin G. NIH 3T3 cells stained intensely for perlecan (A), which is localized mainly in the extracellular spaces outlining the cell boundaries, as can be clearly seen at a higher magnification (B). Mouse perlecan antisense cells (mPAS-1) exhibited markedly reduced staining for perlecan (D), and no perlecan could be detected in the extracellular space even at high magnifications (E). Human melanoma cells, when reacted with a monoclonal anti-human perlecan antibody, stained intensely for perlecan (C); in contrast, perlecan antisense cDNA-transfected melanoma cells exhibited significantly reduced cellular perlecan staining (F). Bars: 25  $\mu\text{m}$  (A and D) and 10  $\mu\text{m}$  (B, C, E, and F).

therefore suggest that the attenuated response to bFGF in cells downregulated for perlecan results primarily from a specific decrease in high-affinity receptor binding.

**Heparin can reconstitute bFGF-receptor binding and affinity labeling in cells expressing perlecan antisense cDNA.** In order to assess whether the observed attenuated bFGF-receptor binding and response of the selected clones is due to their low levels of perlecan-associated HS chains, heparin was used together with bFGF. As demonstrated in Fig. 5A, wild-type and neomycin-resistant NIH 3T3 cells (NIH neo) can bind bFGF at maximal levels, regardless of whether heparin is present. On the other hand, heparin at 5  $\mu\text{g}/\text{ml}$  can specifically enhance high-affinity binding to the clones expressing perlecan at reduced levels. Binding of  $^{125}\text{I}$ -bFGF to the antisense-cDNA-expressing cells performed in the presence of increasing concentrations of heparin demonstrates that heparin can facilitate receptor binding in these cells in a dose-dependent manner, with maximal receptor binding at 5  $\mu\text{g}$  of heparin per ml (Fig. 6). On the other hand, perlecan antisense cDNA-express-

ing cells bind the non-heparin-binding growth factor EGF in the absence as well as in the presence of heparin (Fig. 5C), demonstrating that perlecan antisense cDNA expression does not have any effect on the binding of other, non-perlecan-dependent growth factors.

Affinity labeling of wild-type and perlecan antisense cDNA-transfected cells with  $^{125}\text{I}$ -bFGF carried out in the presence of increasing concentrations of heparin demonstrated the formation of specific bFGF-receptor complexes at heparin concentrations of 5 to 10  $\mu\text{g}/\text{ml}$  (Fig. 7A). This is in good agreement with the direct binding data (Fig. 6). Moreover, a good correlation seems to exist between the extent of residual perlecan expression in each clone (Fig. 2A) and the amount of exogenous heparin required to reconstitute receptor binding, supporting the notion that the marked decrease in receptor binding is due to the lack of HSs capable of promoting high-affinity bFGF-receptor interactions. Identical levels of FGF receptor 1 protein are present in both wild-type and perlecan antisense cDNA-expressing cells, as demonstrated by a Western blot

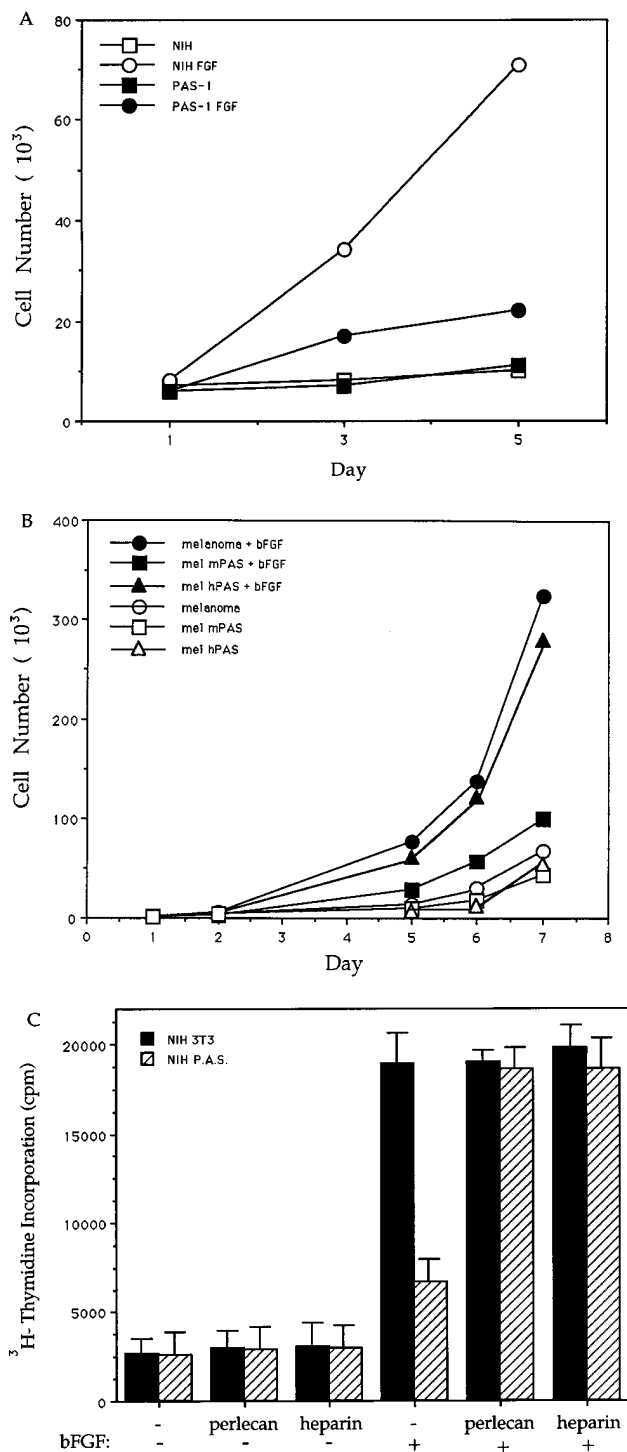


FIG. 4. bFGF-induced cell proliferation of wild-type and perlecan antisense cDNA-expressing NIH 3T3 and human melanoma cells. Wild-type or antisense-cDNA-transfected NIH 3T3 cells (A) and human melanoma (mel) cells, either untransfected or transfected with either mouse (m) or human (h) perlecan antisense constructs (B), were plated at  $2 \times 10^3$  per well in 24-well dishes and grown in the presence or absence of bFGF (10 ng/ml). The cells were counted at the indicated intervals. Values represent mean cell numbers obtained in duplicate in one of two experiments. (C) Effects of heparin and perlecan on the mitogenic responses of wild-type and PAS NIH 3T3 cells to bFGF. Wild-type NIH 3T3 and transfected cells (mPAS-1) were serum starved for 24 h and then incubated with 10 ng of bFGF per ml in the absence (-) or presence (+) of heparin (1  $\mu$ g/ml) or perlecan (100 ng/ml). Mitogenic activity was evaluated by measuring [ $^3$ H]thymidine incorporation into DNA. Values represent mean counts obtained in triplicate in one of two representative experiments. Error bars represent standard deviations.

analysis (Fig. 7B), indicating that the attenuated response in cells downregulated for perlecan is not due to downregulation of the signaling receptors.

## DISCUSSION

Stable overexpression of an antisense perlecan cDNA in NIH 3T3 fibroblasts and in human metastatic melanomas results in downregulation of perlecan protein and inhibition of cellular responses to bFGF. The engineered cells show neither enhanced proliferation nor increased DNA synthesis in response to high concentrations of bFGF, which under the same experimental conditions are capable of inducing a maximal mitogenic response in untransfected cells. We demonstrate that the attenuated ability of bFGF to induce mitogenic activity results from loss of high-affinity binding, which is in turn a direct consequence of their reduced perlecan expression. We have previously shown that perlecan, purified to homogeneity from human fetal lung fibroblasts, can promote heparin-dependent, high-affinity binding of bFGF in vitro and angiogenesis in vivo. It has been recently demonstrated that bFGF binds specifically to HS chains attached to domain I of perlecan isolated from human endothelial cells (40). Taken together, these observations and the current results indicate that perlecan is a major accessory receptor for bFGF, supporting both autocrine and paracrine bFGF receptor-mediated responses.

Cell surface and extracellular matrix resident HSPGs serve as major regulators of heparin-dependent growth factor-receptor interactions as well as efficient large-capacity, short- and long-term backup systems. HSPGs such as syndecan-1 can inhibit bFGF-receptor binding and activation in a dose-dependent manner (1, 26), and overexpression of syndecan-1 in NIH 3T3 cells makes the cells totally resistant to bFGF (19). Thus, either overexpression of an inhibitory HSPG or elimination of an active HSPG can result in the specific suppression of bFGF-mediated cellular responses.

Significant recovery of bFGF binding to perlecan antisense cDNA-expressing cells is achieved only at heparin concentrations of 5  $\mu$ g/ml. This is a relatively high heparin dose compared to that required for inducing receptor binding and activation in HS-deficient cells (1, 32, 42), and it may result from selective elimination of perlecan glycosaminoglycan chains, leaving intact all other proteoglycans, most of which carry bFGF-inhibitory HS sequences (e.g., syndecan-1) (1, 26). Under such unfavorable conditions, higher doses of heparin are required to competitively allow proper heparin-dependent FGF-receptor functional interactions.

HS chains of proteoglycans are organized into widely spaced, highly sulfated structural motifs, and this property may be important for their differential protein-binding activities (10). Direct evidence of alternating FGF-regulating oligosaccharide sequences within a unique HSPG has been obtained by the differential response of neural cells to either FGF-1 or FGF-2 during development, determined by the expression of differentially glycanated forms of a single HSPG (31). Our data support the hypothesis that a balance between different classes of HSPG will determine the character of bFGF-induced cellular responses. This balance can be modulated by different independent mechanisms, including transcriptional, translational, and posttranslational alterations in HSPGs. Both spatial and temporal regulation of bFGF activity can thus be achieved by local overexpression of an active HSPG such as perlecan or a decrease in the expression of bFGF-inhibitory species of HSPG like syndecan-1.

In the course of their adaptation to tissue culture conditions, cells undergo dramatic morphological and functional changes,

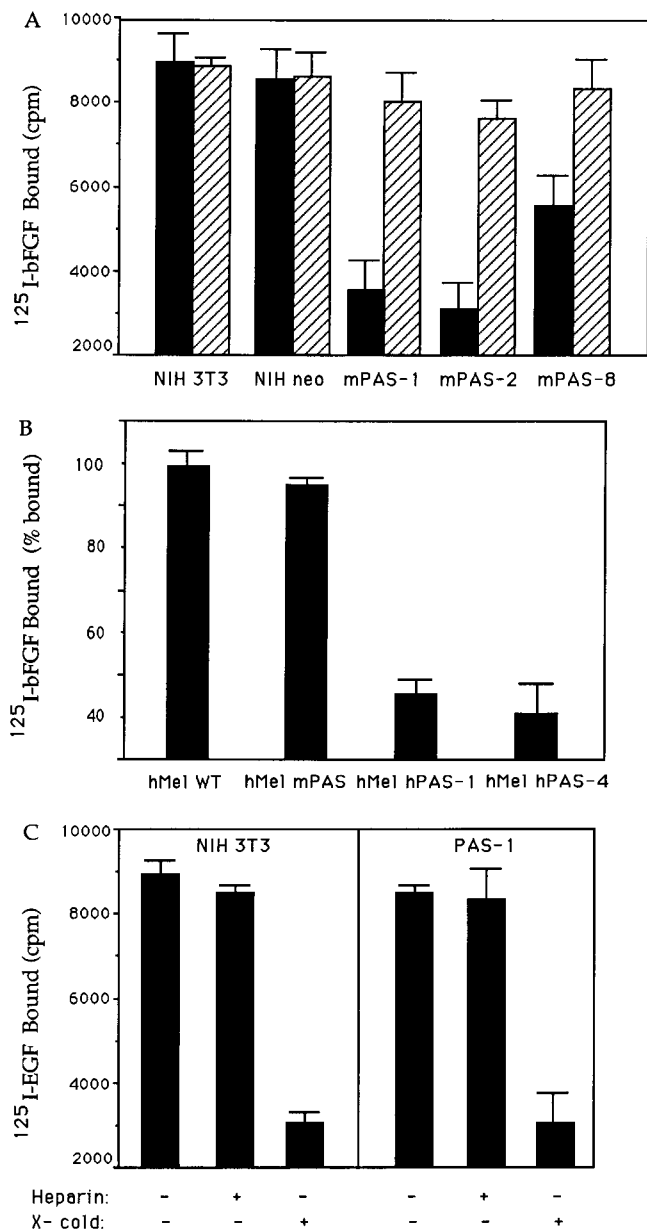


FIG. 5. Effects of perlecan antisense cDNA expression on receptor binding of  $^{125}\text{I}$ -bFGF. (A) Radiolabeled bFGF (2 ng/ml) was incubated with wild-type, neomycin (neo)-resistant, or perlecan antisense cDNA-transfected NIH 3T3 cell lines in the absence (solid bars) or presence (hatched bars) of 5  $\mu\text{g}$  of heparin per ml. (B)  $^{125}\text{I}$ -labeled bFGF (2 ng/ml) was incubated with wild-type and human (h) or mouse (m) perlecan antisense cDNA-transfected human melanoma (hMel) cell lines for 90 min at 4°C. High-affinity-bound ligand was measured upon removal of the low-affinity fraction with 1.6 M NaCl in PBS (pH 7.4). Results represent one of three independent experiments. Nonspecific binding was determined in the presence of a 100-fold excess of unlabeled ligand. (C)  $^{125}\text{I}$ -EGF (1 ng/ml) was incubated with wild-type or perlecan antisense cDNA-transfected NIH 3T3 cell lines for 90 min at 4°C in the absence (-) or presence (+) of 5  $\mu\text{g}$  of heparin per ml. Receptor-bound ligand was measured after extensive washing with PBS (pH 7.4). Nonspecific binding was determined in the presence of a 100-fold excess of unlabeled EGF (x-cold). In all panels, error bars indicate standard deviations.

moving from quiescence to a highly metabolic, proliferative state. One noticeable change is the production of a multitude of growth factors and cytokines capable of supporting autocrine cell growth and survival. FGF expression is highly abundant in cultured cells of both normal and malignant origins. A

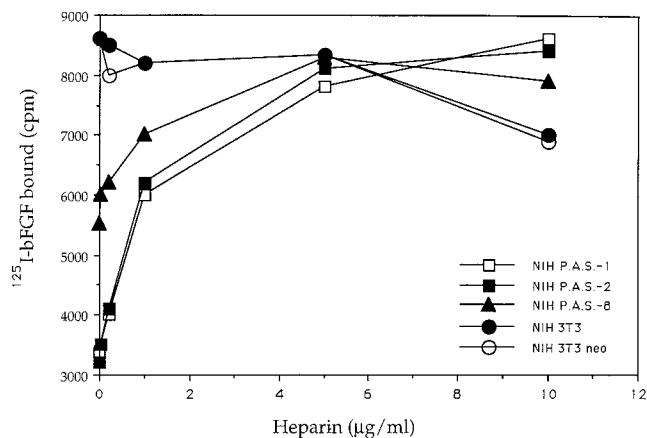


FIG. 6. Dose response of heparin in the binding of bFGF to wild-type and perlecan antisense cDNA-expressing cells. Wild-type or perlecan antisense cDNA-transfected NIH 3T3 cells were incubated with  $^{125}\text{I}$ -bFGF in the absence or presence of increasing concentrations of heparin (1 to 20  $\mu\text{g/ml}$ ), and the amount of specifically bound ligand was determined as described in the text.

recent study has demonstrated that retinal pigmented cells in early passage exhibit low-level perlecan expression and low mitogenic activity in response to bFGF (12). At later passages, the mitogenic response to FGF is highly elevated, in parallel with an increase in cellular perlecan expression. The levels of FGF receptor 1 expression in both early- and late-passage cells were found to be identical, indicating that the marked difference in FGF-induced proliferation between the various stages is not due to alterations in the signaling receptor level. Furthermore, the impaired response of early-passage cells to bFGF could be rescued upon addition of exogenous heparin, indicating that the lack of heparin-like molecules is most probably responsible for the lack of response to bFGF. In light of the critical role of perlecan in FGF signaling, it is most interesting and relevant to note the concomitant increase in perlecan expression in conjunction with the capacity of pigmented cells to respond to exogenous bFGF. Upregulation of both growth factors and their accessory HSPGs may therefore serve as a switch leading to the highly proliferative state of cells during embryonal development and through angiogenesis and malignant transformation.

There is growing evidence for the involvement of perlecan in tumor progression and vascularization. Perlecan is expressed at different levels in normal, benign breast tumors and in in situ carcinomatous breast tissue, where it is found scattered around and surrounding the tumor blood vessels (16). Perlecan is also found to be highly abundant in liver neoplastic nodules (36). A survey of hepatocellular carcinomas indicated that there is a 20-fold increase in glycosaminoglycan content in the malignant tissue in comparison to that in normal liver. Interestingly, the amount of perlecan in liver carcinomas is specifically elevated while syndecan-1 protein is dramatically downregulated (23), suggesting that malignant transformation in the liver is accompanied by specific alterations in the content, composition, and structure of HSPG.

It is well established that while normal melanocytes require exogenous bFGF for proliferation in vitro, metastatic melanomas produce bFGF and can grow in protein-free medium (8). Moreover, proliferation of human malignant melanomas is inhibited by antisense oligonucleotides targeted against bFGF (4). These observations strongly suggest that melanoma tumor progression is supported by an endogenous autocrine loop of bFGF (15). Human metastatic melanomas express high levels

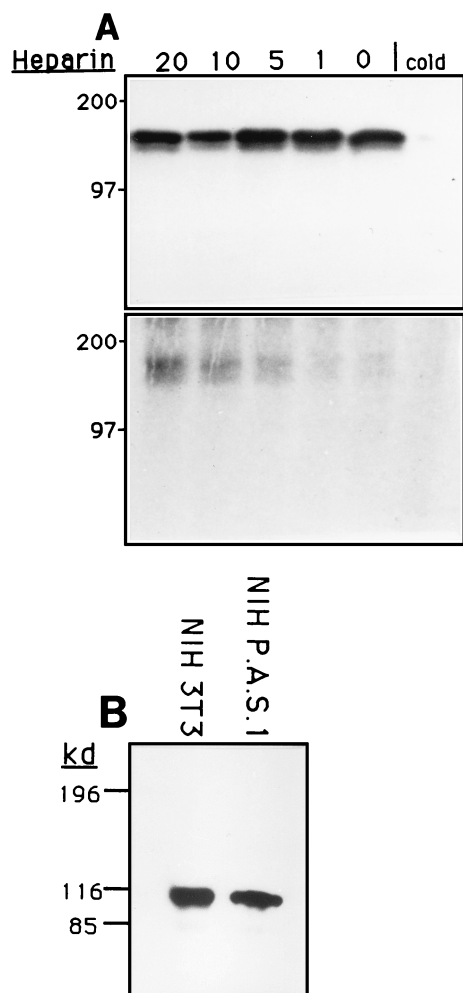


FIG. 7. Chemical cross-linking of  $^{125}\text{I}$ -bFGF to wild-type and perlecan antisense cDNA-expressing cells. (A) Affinity labeling of cells with  $^{125}\text{I}$ -bFGF as a function of heparin concentration (in micrograms per milliliter). Receptor-bound  $^{125}\text{I}$ -bFGF complexes were subjected to cross-linking, SDS-polyacrylamide gel electrophoresis, and autoradiography. Nonspecific binding was determined in the presence of a 100-fold excess of unlabeled bFGF (cold). Upper panel, wild-type NIH 3T3; lower panel, NIH mPAS-1. (B) Western blot analysis of FGF receptors. Total cell lysates of wild-type and PAS-transfected NIH 3T3 clones were concentrated on wheat germ agglutinin beads, separated on an SDS-7.5% polyacrylamide gel, transferred to nitrocellulose, and reacted with rabbit antiserum generated against mouse FGF receptor 1.

of perlecan (7), and downmodulation of perlecan by antisense constructs inhibits bFGF-induced proliferation of human melanoma cells. The dramatic effect of perlecan downregulation on human melanoma cells also reemphasizes the potential autocrine function of endogenously expressed bFGF in melanoma growth and survival. Taken together, these observations support the notion that perlecan may be directly involved in FGF functions in melanocytes (15, 21) and that it plays a key role in the multifactorial etiology of metastatic melanomas.

The ubiquitous expression of bFGF and its receptors in normal cells and tissues demands both temporal and spatial tight regulation through fine tuning of their molecular interactions. The coordinated expression of bFGF and perlecan and their cooperative functioning may have a key role in this fine tuning as well as in the switch to rapid cell proliferation typical of tumor progression and angiogenesis. Perlecan may therefore play a pivotal role in bFGF receptor signaling, for which

its presence in the cellular microenvironment seems to be crucial within specific cells for the appropriate paracrine and autocrine activities of bFGF.

#### ACKNOWLEDGMENTS

This work was supported in part by the Israel Academy of Science and Humanities, the Israel Cancer Research Fund (I.C.R.F.) (A.Y.), the Clore Foundation award (D.A.), and the Associazione Italiana per la Ricerca sul Cancro (D.M.N.).

We thank Tova Shimon for excellent technical assistance, Koji Kimata and Guido David for the perlecan protein and antibodies, Merton Bernfield for the syndecan-1 antibodies, Rina Zakut for the human cell lines, and Polina Goichberg for her help in immunohistochemical analysis.

#### REFERENCES

- Aviezer, D., E. Levy, M. Safran, C. Svahn, E. Buddecke, A. Schmidt, G. David, I. Vlodavsky, and A. Yayon. 1994. Differential structural requirements of heparin and heparan sulfate proteoglycans that promote binding of basic fibroblast growth factor to its receptor. *J. Biol. Chem.* **269**:114-121.
- Aviezer, D., D. Hecht, M. Safran, M. Eisinger, G. David, and A. Yayon. 1994. Perlecan, basal lamina proteoglycan promotes bFGF-receptor binding, mitogenesis and angiogenesis. *Cell* **79**:1005-1013.
- Basilico, C., and D. Moscatelli. 1992. The FGF family of growth factors and oncogenes. *Adv. Cancer Res.* **159**:115-165.
- Becker, D., C. B. Meier, and M. Herlyn. 1989. Proliferation of human malignant melanomas is inhibited by antisense oligodeoxynucleotides targeted against basic fibroblast growth factor. *EMBO J.* **8**:3685-3691.
- Brickman, Y. G., M. D. Ford, D. H. Small, P. F. Bartlett, and V. Nurcombe. 1995. Heparan sulfates mediate the binding of basic fibroblast growth factor to a specific receptor on neural precursor cells. *J. Biol. Chem.* **270**:24941-24948.
- Chakravarti, S., T. Horchar, B. Jefferson, G. W. Laurie, and J. R. Hassell. 1995. Recombinant domain III of perlecan promotes cell attachment through its RGDS sequence. *J. Biol. Chem.* **270**:404-409.
- Cohen, I. R., A. D. Murdoch, M. F. Naso, D. Marchetti, D. Berd, and R. V. Iozzo. 1994. Abnormal expression of perlecan proteoglycan in metastatic melanomas. *Cancer Res.* **54**:5771-5774.
- Dotto, P. G., G. Moellmann, S. Gosh, M. Edwards, and R. Halaban. 1989. Transformation of murine melanocytes by bFGF cDNA and oncogenes and selective suppression of the transformed phenotype in a reconstituted cutaneous environment. *J. Cell Biol.* **109**:3115-3128.
- Folkman, J., and Y. Shing. 1992. Control of angiogenesis by heparin and other sulfated polysaccharides. *Adv. Exp. Med. Biol.* **313**:355-364.
- Gallagher, J. T. 1994. Heparan sulphates as membrane receptors for the fibroblast growth factors. *Eur. J. Clin. Chem. Clin. Biochem.* **32**:239-247.
- Guelstein, V. I., T. A. Tchypysheva, V. D. Ermilova, and A. V. Ljubimov. 1993. Myoepithelial and basement membrane antigens in benign and malignant human breast tumors. *Int. J. Cancer* **53**:269-277.
- Guillonnet, X., J. Tassin, E. Berrou, M. Bryckaert, Y. Courtois, and F. Mascarelli. 1996. In vitro changes in plasma membrane heparan sulfate proteoglycans and in perlecan expression participate in the regulation of fibroblast growth factor 2 mitogenic activity. *J. Cell. Physiol.* **166**:170-187.
- Guimond, S., M. Maccarana, B. B. Olwin, U. Lindahl, and A. C. Rapraeger. 1993. Activating and inhibitory heparin sequences for FGF-2 (basic FGF). Distinct requirements for FGF-1, FGF-2, and FGF-4. *J. Biol. Chem.* **268**:23906-23914.
- Gunning, P., J. Leavitt, G. Muscat, S. Y. Nig, and L. Keddes. 1987. Differential patterns of transcript accumulation during human myogenesis. *Proc. Natl. Acad. Sci. USA* **84**:4831-4835.
- Halaban, R., B. S. Kwon, S. Ghosh, P. Delli Bovi, and A. Baird. 1988. bFGF as an autocrine growth factor for human melanomas. *Oncogene Res.* **3**:177-186.
- Iozzo, R. V., I. R. Cohen, S. Grassel, and A. D. Murdoch. 1994. The biology of perlecan: the multifaceted heparan sulphate proteoglycan of basement membranes and pericellular matrices. *Biochem. J.* **302**:625-639.
- Iozzo, R. V. 1984. Biosynthesis of heparan sulfate proteoglycan by human colon carcinoma cells and its localization at the cell surface. *J. Cell Biol.* **99**:403-417.
- Ishihara, M. 1994. Structural requirements in heparin for binding and activation of FGF-1 and FGF-4 are different from that for FGF-2. *Glycobiology* **4**:817-824.
- Jalkanen, M., A. Määttä, T. Vihinen, and P. Jaakkola. 1995. Syndecan-1 in growth factor action: an inhibitory loop for FGF-function, p. 17. *In Abstracts of the EMBO/NORFA Workshop on Growth Factors and Receptor Kinases*, Helsinki, Finland.
- Kato, M., Y. Koike, S. Suzuki, and K. Kimata. 1988. Basement membrane proteoglycan in various tissues: characterization using monoclonal antibodies to the Engelbreth-Holm-Swarm mouse tumor low density heparan sulfate



- proteoglycan. *J. Cell Biol.* **106**:2203–2210.
21. **Klagsbrun, M.** 1989. The fibroblast growth factor family: structural and biological properties. *Prog. Growth Factor Res.* **1**:207–235.
  22. **Kokenyesi, R., and J. E. Silbert.** 1995. Formation of heparan sulfate or chondroitin/dermatan sulfate on recombinant domain I of mouse perlecan expressed in Chinese hamster ovary cells. *Biochem. Biophys. Res. Commun.* **211**:262–267.
  23. **Kovalszky, I., Z. Schaff, and A. Jeney.** 1993. Potential markers (enzymes, proteoglycans) for human liver tumors. *Acta Biomed. Ateneo Parmense* **64**:157–163.
  24. **Laslett, A. L., J. R. McFarlane, M. T. Hearn, and G. P. Risbridger.** 1995. Requirement for heparan sulphate proteoglycans to mediate basic fibroblast growth factor (FGF-2)-induced stimulation of Leydig cell steroidogenesis. *J. Steroid Biochem. Mol. Biol.* **54**:245–250.
  25. **Maccarana, M., B. Casu, and U. Lindahl.** 1993. Minimal sequence in heparin/heparan sulfate required for binding of basic fibroblast growth factor. *J. Biol. Chem.* **268**:23898–23905.
  26. **Mali, M., K. Elenius, H. M. Miettinen, and M. Jalkanen.** 1993. Inhibition of basic fibroblast growth factor-induced growth promotion by overexpression of syndecan-1. *J. Biol. Chem.* **268**:24215–24222.
  27. **Mansukhani, A., P. Dell'Era, D. Moscatelli, S. Kornbluth, H. Hanafusa, and C. Basilico.** 1992. Characterization of the murine BEK fibroblast growth factor (FGF) receptor: activation by three members of the FGF family and requirement for heparin. *Proc. Natl. Acad. Sci. USA* **89**:3305–3309.
  28. **Mathieu, M., E. Chatelain, D. Ornitz, J. Bresnick, I. Mason, P. Kiefer, and C. Dickson.** 1995. Receptor binding and mitogenic properties of mouse fibroblast growth factor 3. Modulation of response by heparin. *J. Biol. Chem.* **270**:24197–24203.
  29. **Murdoch, A. D., G. R. Dodge, I. Cohen, R. S. Tuan, and R. V. Iozzo.** 1992. Primary structure of the human heparan sulfate proteoglycan from basement membrane (HSPG2/perlecan). A chimeric molecule with multiple domains homologous to the low density lipoprotein receptor, laminin, neural cell adhesion molecules, and epidermal growth factor. *J. Biol. Chem.* **267**:8544–8557.
  30. **Noonan, D. M., A. Fulle, P. Valente, S. Cai, E. Horigan, M. Sasaki, Y. Yamada, and J. R. Hassell.** 1991. The complete sequence of perlecan, a basement membrane heparan sulfate proteoglycan, reveals extensive similarity with laminin A chain, low density lipoprotein receptor, and the neural cell adhesion molecule. *J. Biol. Chem.* **266**:22939–22947.
  31. **Nurcombe, V., M. D. Ford, J. A. Wildschut, and P. F. Bartlett.** 1993. Developmental regulation of neural response to FGF-1 and FGF-2 by heparan sulfate proteoglycan. *Science* **260**:103–106.
  32. **Ornitz, D. M., A. Yayon, J. G. Flanagan, C. M. Svahn, E. Levi, and P. Leder.** 1992. Heparin is required for cell-free binding of basic fibroblast growth factor to a soluble receptor and for mitogenesis in whole cells. *Mol. Cell Biol.* **12**:240–247.
  33. **Pantoliano, M. W., R. A. Horlick, B. A. Springer, D. D. Van, T. Tobery, D. R. Wetmore, J. D. Lear, A. T. Nahapetian, J. D. Bradley, and W. P. Sisk.** 1994. Multivalent ligand-receptor binding interactions in the fibroblast growth factor system produce a cooperative growth factor and heparin mechanism for receptor dimerization. *Biochemistry* **33**:10229–10248.
  34. **Rapraeger, A. C., S. Guimond, A. Krufka, and B. B. Olwin.** 1994. Regulation by heparan sulfate in fibroblast growth factor signaling. *Methods Enzymol.* **245**:219–240.
  35. **Rapraeger, A. C., A. Krufka, and B. B. Olwin.** 1991. Requirement of heparan sulfate for bFGF-mediated fibroblast growth and myoblast differentiation. *Science* **252**:1705–1707.
  36. **Rescan, P. Y., O. Loreal, J. R. Hassell, Y. Yamada, A. Guillouzo, and B. Clement.** 1993. Distribution and origin of the basement membrane component perlecan in rat liver and primary hepatocyte culture. *Am. J. Pathol.* **142**:199–208.
  37. **Saunders, S., M. Jalkanen, S. O'Farrell, and M. Bernfield.** 1989. Molecular cloning of syndecan, an integral membrane proteoglycan. *J. Cell Biol.* **108**:1547–1556.
  38. **Spivak, K. T., M. A. Lemmon, I. Dikic, J. E. Ladbury, D. Pinchasi, J. Huang, M. Jaye, J. Schlessinger, and I. Lax.** 1994. Heparin-induced oligomerization of FGF molecules is responsible for FGF receptor dimerization, activation, and cell proliferation. *Cell* **79**:1015–1024.
  39. **Walker, A., J. E. Turnbull, and J. T. Gallagher.** 1994. Specific heparan sulfate saccharides mediate the activity of basic fibroblast growth factor. *J. Biol. Chem.* **269**:931–935.
  40. **Whitlock, J. M., A. D. Murdoch, R. V. Iozzo, and A. P. Underwood.** 1996. The degradation of human endothelial cell-derived perlecan and release of bound bFGF by stromelysin, collagenase, plasmin and heparanases. *J. Biol. Chem.* **271**:10079–10086.
  41. **Yayon, A., and M. Klagsbrun.** 1990. Autocrine regulation of cell growth and transformation by basic fibroblast growth factor. *Cancer Metastasis Rev.* **9**:191–202.
  42. **Yayon, A., M. Klagsbrun, J. D. Esko, P. Leder, and D. M. Ornitz.** 1991. Cell surface, heparin-like molecules are required for binding of basic fibroblast growth factor to its high affinity receptor. *Cell* **64**:841–848.
  43. **Zakut, R., R. Perlis, S. Eliyahu, Y. Yarden, D. Givol, S. D. Lyman, and R. Halaban.** 1993. KIT ligand (mast cell growth factor) inhibits the growth of KIT-expressing melanoma cells. *Oncogene* **8**:2221–2229.